JOURNAL OF COMPUTATIONAL PHYSICS 73, 244–266 (1987)

Parasitic Waves and Solitons in the Numerical Solution of the Korteweg–de Vries and Modified Korteweg–de Vries Equation

M. F. MARITZ AND S. W. SCHOOMBIE

Department of Applied Mathematics, University of the Orange Free State, Bloemfontein, South Africa

Received January 22, 1986; revised October 1, 1986

By means of numerical experiments, the Zabusky–Kruskal discretization of the Korteweg de Vries equation, is shown to have solitary saw-toothed wave packet solutions. An analysis is presented to explain the properties of this type of solution. This, as well as numerical experiments indicate that the solution is stable only for small amplitude wave packets and that the propagation of the wave packet is essentially linear. Similar experiments and analysis for a discretized modified-Korteweg–de Vries equation show that large amplitude solitary wave packet solutions are possible for this equation and that their propagation is governed by an MKdV equation which differs from the one which is consistent with the discretized equation. This makes it possible to construct sawtoothed wave packets which behave like MKdV-solitons. The results of several numerical experiments showing collisions between wave packets and solitons are also reported. © 1987 Academic Press, Inc.

1. INTRODUCTION

Parasitic waves or nonphysical waves occurring in the numerical solution of certain wave equations can be due to several causes. In some cases such spurious waves are caused by the use of high order difference methods, and they can then often be filtered out by applying suitable difference operators to the initial data (Hedstrom [1], Schoombie [2]). We shall not be concerned with these in this paper.

In other cases, such parasitic waves are observed in the numerical solution when discontinuities in the coefficients of the differential equation or in the initial data are present. In these cases such waves correspond to high wave numbers and are the effect of numerical dispersion, as was pointed out by Trefethen [3–5], and Giles and Thompkins [6]. These authors only considered the numerical solution of non-dispersive, *linear* wave equations, so that the only dispersion is that introduced by discretization.

In this paper we wish to report some related phenomena observed in

0021-9991/87 $3.00

the numerical solution of nonlinear, dispersive wave equations such as the Korteweg–de Vries (KdV) equation

$$u_t + \eta u_x + \rho u u_x + \varepsilon u_{xxx} = 0 \tag{1.1}$$

and the modified Korteweg–de Vries (MKdV) equation

$$u_t + \eta u_x + \rho u^2 u_x + \varepsilon u_{xxx} = 0. \tag{1.2}$$

When either (1.1) or (1.2) are solved with a rectangular pulse initial condition, solitons will emerge, as well as a dispersive trial moving in the opposite direction [7, 9]. When using a central difference method such as that of Zabusky and Kruskal [8] to solve (1.1) or (1.2) numerically, an additional wave train corresponding to high wave numbers is seen to emerge, moving in the same direction and ahead of the solitons. This is again at least partly due to numerical dispersion, as will be shown. For certain combinations of the coefficients in (1.1) as well as gridlength a solitary wave packet was seen to emerge instead of a parasitic wave train. We shall present an analysis which indicates that sawtoothed wave packets with a well-defined smooth envelope cannot exist as solutions of the Zabusky–Kruskal scheme for (1.1), unless their amplitudes are small enough for the effect of the nonlinear terms to be negligible. This is confirmed by numerical experiments in which such wave packets become unstable whenever their amplitudes are made too large. Thus these small wave packets behave very much like linear modulations, with envelopes moving along at the linear group velocity corresponding to saw-toothed waves. In the case of (1.2), wave packets with smooth envelopes and larger amplitudes cannot only exist, but can be shown to have envelopes satisfying approximately an MKdV-equation *different* from (1.2). Thus the envelopes can be expected to behave approximately like solitons, and in fact we found that typical soliton interactions between such wave packets are possible. However, we have not yet been able to observe such a single wave packet to emerge from rectangular pulse initial conditions in the case of (1.2). The remarkable thing here is, nevertheless, that the difference scheme for (1.2) can have soliton solutions (or at least near-soliton solutions) which differ considerably from those of the original differential equation.

In Section 2 we discuss the effect of numerical dispersion in the case of the linearized version of (1.1) and (1.2) (i.e., $\rho = 0$). We then report the results of some numerical experiments for the nonlinear case, and show that some of the results of the linear analysis are still applicable. In Section 3 we use Taylor series expansions to examine the properties of the envelopes of solitary saw-toothed wave packets in the numerical solutions of (1.1) and (1.2). In Section 4 we discuss the results of numerical experiments in which these wave packets are allowed to interact with solitons. We also show that in the case of (1.2) a two-soliton interaction is possible between two wave packets, depending on the form of the envelopes and the phase difference between the wave packets. The paper is concluded with some general remarks in Section 5.

2. Parasitic Waves Emerging from Discontinuous Data

Let us consider the KdV equation in the form

$$u_t + \eta u_x + \rho u u_x + \varepsilon u_{xxx} = 0 \tag{2.1}$$

with a periodic initial condition

$$u(x, 0) = f(x), \tag{2.2}$$

with f bounded and b-periodic and with the periodic conditions on u

$$u(x, t) = u(x + b, t) \qquad \text{for all} \quad t \geqslant 0. \tag{2.3}$$

We shall also assume the constants ρ and ε to be nonnegative. Contrary to the usual practice of transforming the convective term ηu_x away by means of a Galilean transformation, we shall retain it for the purposes of this study.

For the numerical solution of (2.1) we use the well-known Zabusky–Kruskal leapfrog scheme [8], which makes use of central differences in both time and space. We shall use the following notation: Let τ and h be the timestep and gridlength, respectively, and let U_j^n be the numerical approximation to $u(hj, \tau n)$. Let E_j and E_n be the shift operators defined by

$$E_j U_j^n = U_{j+1}^n, \qquad E_n U_j^n = U_j^{n+1}.$$

We shall then require the following difference operators:

$$\Delta_r = E_r - 1, \qquad \nabla_r = 1 - E_r^{-1},$$

$$\delta_r = E_r - E_r^{-1} = \Delta_r + \nabla_r, \qquad \text{and} \qquad \mu_r = (E_r + 1 + E_r^{-1})/3,$$

where $r = j, n$.

The Zabusky–Kruskal scheme for (1.1) can then be expressed as

$$\delta_n U_j^n + (\eta\tau/h)\,\delta_j U_j^n + (\rho\tau/3h)(\mu_j U_j^n)(\delta_j U_j^n) + (\varepsilon\tau/h^3)\,\delta_j \Delta_j \nabla_j U_j^n = 0$$
$$n = 1, 2, 3, \ldots. \tag{2.4}$$

Because of the leapfrog time differencing, a starter scheme is needed for (2.4). For this purpose we shall, in the case where $n = 0$, replace the term $\delta_n U_j^n$ in (2.4) by $2\Delta_n U_j^n$, thus using a forward Euler integration in time initially.

The scheme (2.4) conserves discrete momentum (i.e., the quantity $\sum_j h U_j^n$) exactly, and it conserves discrete energy (i.e., $\sum_j h(U_j^n)^2$) in the limit $\tau \to 0$) [10]. The linear stability condition for (2.4) is [10, 11]

$$\{\tau(\eta + \rho|u|_{\max}) \leqslant h\} \cap \{3\sqrt{3}\,\varepsilon\tau \leqslant 2h^3\}. \tag{2.5}$$

Thus a very small time step is required for stability, which is why other schemes for

the KdV are often preferred [12, 13]. In this paper, however, we shall be primarily be concerned with certain effects due to the *spacial* discretization, so that the use of small time steps would actually suit our purpose.

We shall use the following rectangular pulse initial condition:

$$f(x)=\begin{cases} 0 & \text{when} \quad 0\leqslant x<d_0 \\ H & \text{when} \quad d_0\leqslant x\leqslant d_1 \\ 0 & \text{when} \quad d_1<x<b. \end{cases} \tag{2.6}$$

2.1. *Linear Case*

Before we can consider the nonlinear case $\rho\neq 0$, we first wish to point out the effects due to the linear terms in (2.1) and (2.4). Using standard Fourier techniques, the solution of (2.1) and (2.2), when $\rho=0$, taking into account (2.3) and (2.6), can also be written as

$$\begin{aligned} u(x,t) &= (2H/b)\sum_{p=-\infty}^{\infty}\{\sin[K_p(d_1-d_1)/2]/K_p\}\exp\{i[K_p(x-\bar{x})-\omega(K_p)\,t]\} \\ &= H(d_1-d_0)/b+(4H/b)\sum_{p=1}^{\infty}\{\sin[K_p(d_1-d_0)/2]/K_p\}\cos[K_p(x-\bar{x})-\omega(K_p)\,t], \end{aligned} \tag{2.7}$$

where

$$K_p=2\pi p/b \tag{2.8a}$$

$$\bar{x}=(d_1+d_2)/2 \tag{2.8b}$$

$$\omega(K_p)=\eta K_p-\varepsilon K_p^3 \tag{2.8c}$$

$$\lambda(K_p)=2\pi/K_p=b/p. \tag{2.8d}$$

Here K_p is the wave number of the pth Fourier-mode, and (2.8c) is the dispersion relation. $\lambda(K_p)$ is the wave length of this node. The phase velocity of the node with wave number K_p is

$$c(K_p)=\omega(K_p)/K_p=\eta-\varepsilon K_p^2. \tag{2.9}$$

The group velocity is

$$C(K_p)=\frac{d\omega}{dK_p}=\eta-3\varepsilon K_p^2. \tag{2.10}$$

Thus the modes with low wave numbers will have large amplitudes and will move in the positive x-direction, with velocity less than η. Modes with higher wave-numbers ($K_p>(\eta/\varepsilon)^{1/2}$) will have small amplitudes and will move in the negative x-direction. If $\eta=0$ *all* modes will move in the negative x-direction.

It is interesting to compare these results with the solution of the numerical scheme (2.4), which contains some numerical dispersion in addition to the dispersion inherent to Eq. (2.1).

Let $N = b/h$ be the even number of subintervals into which the interval $[0, b]$ is divided by the nodes $x_j = b/2 + hj = (N/2 + j)\,h$, $j = -N/2,\ldots, N/2$. Let furthermore $\hat{U}_p^n$ be the discrete Fourier transform of U_j^n, defined by

$$\begin{aligned}\hat{U}_p^n &= (h/b) \sum_{j=-N/2}^{N/2-1} U_j^n \exp[-i(2\pi p/b)(x_j - b/2)] \\ &= (1/N) \sum_{j=-N/2}^{N/2-1} U_j^n \exp[-i(2\pi pj/N)] \end{aligned} \tag{2.11}$$

with the inverse Fourier transform given by

$$\begin{aligned} U_j^n &= \sum_{p=-N/2}^{N/2-1} \hat{U}_p^n \exp[i(2\pi pj/N)] \\ &= \sum_{p=-N/2}^{N/2-1} \hat{U}_p^n \exp[i(2\pi p/b)(x_j - b/2)]. \end{aligned} \tag{2.12}$$

Since the discrete Fourier transform of $(E_j)^k U_j^n$ is $\hat{U}_p^n \exp[i(2\pi pk/N]$, we can take the discrete Fourier transform of the scheme (2.4), thus obtaining an expression for $\hat{U}_p^n$ in the form

$$\hat{U}_p^n = A_p \exp(-in\tau\omega_h(K_p)) + (-1)^n B_p \exp(in\tau\omega_h(K_p)) \quad \text{for} \quad n = 2, 3,\ldots, \tag{2.13}$$

where

$$(h/\tau)\sin(\omega_h(K_p)\,\tau) = [\eta - 2\varepsilon/h^2]\sin(K_p h) + (\varepsilon/h^2)\sin(2K_p h) \tag{2.14a}$$

and

$$K_p = 2\pi p/b. \tag{2.14b}$$

Also, taking the discrete Fourier transform of the scheme (2.4) with the Euler starter at $n = 0$, it is seen that

$$\hat{U}_p^1 = [1 - i\sin(\tau\omega_h(K_p))]\,\hat{U}_p^0. \tag{2.15}$$

Taking, for $j = -N/2,\ldots, N/2 - 1$, $U_j^0 = H$ when $j_0 \leqslant j \leqslant j_1$ and zero otherwise, with $d_r = b/2 + hj_r$, $r = 0, 1$, it is possible to calculate $\hat{U}_p^0$ from (2.11), and from (2.13) and (2.15) A_p and B_p can then be found.

Finally, using (2.12), it is seen that

$$U_j^n = (H/b)(d_1 - d_0 + h) + \sum_{p=1}^{N/2} a(K_p)[1 - f(K_p)] \cos[K_p(x_j - \bar{x}) - \omega_h(K_p)\, t_n]$$
$$+ (-1)^n \sum_{p=1}^{N/2-1} a(K_p)\, f(K_p) \cos[K_p(x_j - \bar{x}) + \omega_h(K_p)\, t_n], \tag{2.16a}$$

where

$$\bar{x} = (d_1 + d_0)/2, \qquad t_n = n\tau, \tag{2.16b}$$

$$a(K_p) = \{\sin[K_p(d_1 - d_0 + h)/2]/\sin(K_p h/2)\} \times \begin{cases} 2Hh/b & \text{for } p \neq N/2 \\ Hh/b & \text{for } p = N/2 \end{cases} \tag{2.16c}$$

and

$$f(K_p) = (1 - \sec(\omega_h(K_p)\, \tau))/2 \tag{2.17}$$

and where it is assumed that j_1 and j_0 are either both even or both odd so that $\sin[(\pi/h)(x_j - \bar{x})] = 0$ for all j. Now

$$f(K_p) = -(\omega_h(K_p)\, \tau)^2/4 + O(|\omega_h(K_p)\, \tau|^4) \tag{2.18}$$

and, furthermore, $\omega_h(K_p)$ stays finite if $\tau \to 0$, so that $f(K_p) = O(\tau^2)$ if $\tau \to 0$. Thus every mode in the first summation corresponds to a parasitic mode in the second summation with the same wave length and frequency, moving in the opposite direction, and with amplitude of $O(\tau^2)$.

In practice τ has to be taken very small in any case, to satisfy the linear stability conditions (2.5), so that these $O(\tau^2)$ parasitic waves can be ignored—they do not figure significantly in numerical computations.

Thus assuming that we neglect $O(\tau^2)$ quantities, (2.16a) reduces to

$$U_j^n = (H/b)(d_1 - d_0 + h) + \sum_{p=1}^{N/2} a(K_p) \cos[K_p(x_j - \bar{x}) - \omega_h(K_p)\, t_n]. \tag{2.19}$$

This is very similar to the analytic solution (2.7), except that there are now only $N/2 + 1$ distinct modes, the amplitudes of modes with corresponding wavenumbers are different, especially for high wavenumbers, and the dispersion relation is (2.14a) instead of (2.8c).

Since we are neglecting $O(\tau^2)$ quantities, (2.14a) can be rewritten in the form

$$h\omega_h(K_p) = [\eta - 2\varepsilon/h^2] \sin(K_p h) + (\varepsilon/h^2) \sin(2K_p h). \tag{2.20}$$

For the mode with wavenumber K_p the phase velocity is

$$c_h(K_p) = \omega_h(K_p)/K_p = [\eta - 2\varepsilon/h^2][\sin(K_p h)/(K_p h)] + (2\varepsilon/h^2)[\sin(2K_p h)/(2K_p h)] \tag{2.21}$$

and the group velocity is

$$C_h(K_p) = \frac{d\omega_h(K_p)}{dK_p} = [\eta - 2\varepsilon/h^2]\cos(K_p h) + (2\varepsilon/h^2)\cos(2K_p h). \tag{2.22}$$

It can easily be seen that

$$\begin{aligned} \omega_h(K_p) &= \omega(K_p) + O(K_p^2 h^2) \\ c_h(K_p) &= c(K_p) + O(K_p^2 h^2) \\ C_h(K_p) &= C(K_p) + O(K_p^2 h^2) \end{aligned} \tag{2.23}$$

and

$$a(K_p) = (4H/b)[\sin\{K_p(d_1 - d_0)/2\}/K_p] + O(K_p h) \qquad \text{if} \quad K_p, h \to 0,$$

so that the modes with low wavenumbers correspond well with their counterparts in the analytic solution (2.7). The modes with higher wavenumbers show marked differences, however. The highest possible wavenumber in (2.19) is $K_{N/2} = \pi/h$, corresponding to a saw-toothed wave with wavelength $2h$. In this case

$$c_h(\pi/h) = 0 \tag{2.24a}$$

$$C_h(\pi/h) = -\eta + 4\varepsilon/h^2 \tag{2.24b}$$

$$a(\pi/h) = (Hh/b)(-1)^{(d_1 - d_0)/h}. \tag{2.24c}$$

Trefethen [3] and Giles and Thompkins [6] showed that discontinuities in the differential equation or data generally causes a modulated wavetrain of high wave number to emerge in the numerical solution, with the wave front moving along at the *group* velocity C_h. It is expected that this could happen in the present case as well. For simplicity, take $\eta = 0$. Then it is seen from (2.24) that the wavefront of such a saw-toothed parasitic wave will move in the positive x-direction at a group velocity of $4\varepsilon/h^2$. (Note that, from (2.10), *all* modes will move in the *negative* x-direction if $\eta = 0$.) Figure 1 shows some of the results when the numerical scheme (2.4) is applied in the case $\eta = \rho = 0$. The parameters used are as follows:

$H = 1.0 \qquad d_0 = 1.5 \qquad d_1 = 2.5 \qquad b = 6.0 \qquad \varepsilon = 0.0005 \qquad N = 150 \qquad \tau = 0.001$

A graph of the solution was drawn every 300 time steps to the 1200th time step. Each graph is shown for the intervals $x \in [0.,6.]$ and $U \in [-0.3, 1.3]$. Besides a dispersive wave moving towards the left, a modulated saw-toothed wavetrain is clearly seen to emerge towards the right.

2.2. *Nonlinear Case*

Having a clear idea of the effect of dispersion in both (2.1) and (2.4), we now proceed to the nonlinear case where $\rho \neq 0$. Analysis of the analytical solution now

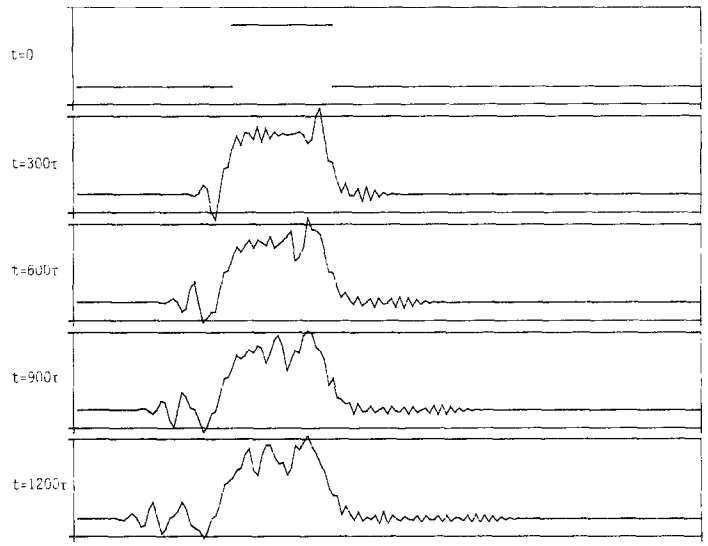

FIG. 1. Numerical solution of KdV-equation, scheme (2.4) with $\eta = 0$, $\rho = 0$, $\varepsilon = 0.0005$, $N = 150$, $h = 0.4$, and $\tau = 0.001$. Initial condition: (2.6) with $H = 1.0$, $d_0 = 1.5$, $d_1 = 2.5$, and $b = 6.0$.

requires techniques such as the inverse scattering transform [7, 9]. Using this technique, it is possible to show that a number of solitons will emerge from a rectangular pulse initial condition, moving towards the right. In addition, a dispersive trail will emerge travelling to the left [7, 9]. No convincing attempt has so far been made to analyze the numerical solution of (2.1). We shall thus only report the results of some numerical experiments, and show in Section 3, how some special types of solutions may be treated analytically.

When using the same parameters as those used to generate Fig. 1, but with $\rho = 1$, a very interesting phenomenon is observed. Figure 2 shows the results. A graph was drawn every 400 time steps from the 0th to the 1600th time step. Each graph is shown on the intervals $x \in [0.0, 6.0]$ and $U \in [-0.3, 1.6]$. Solitons are appearing, as expected, but instead of a modulated saw-toothed parasitic wave emerging, moving towards the right, a single, localized wavepacket is observed, moving towards the right. This wavepacket moves at a speed very near to the group velocity of $4\varepsilon/h^2$ of the saw-toothed parasitic wave in the linear case.

A number of experiments were done to investigate the effect of the height of the initial pulse (H in (2.6)) on the amplitude of the emanating wavepacket. Choosing the same parameters as those used for Fig. 2, and varying H, the maximum amplitude of the wavepacket was measured in each case. The results are recorded in Table I and shown graphically in Fig. 3.

For small H the amplitude of the wavepacket increases more or less linearly with H, but for larger values of H the graph deviates sharply from a straight line. This is not unexpected. From (2.19) it is seen that the amplitude of the emerging wavetrain

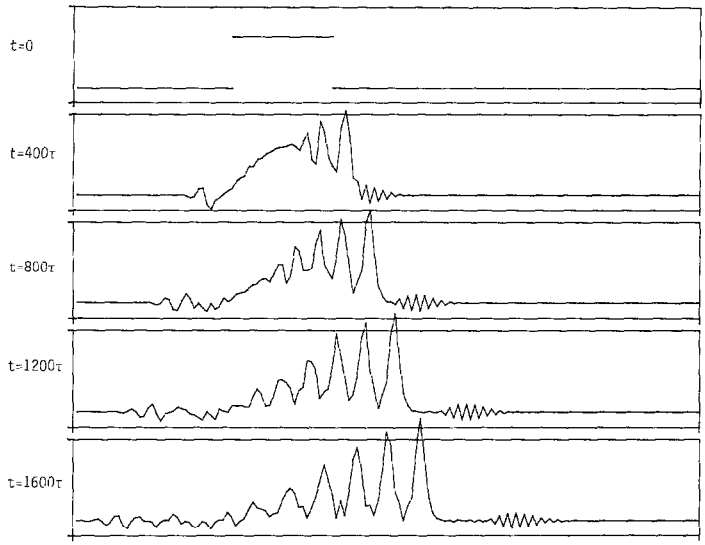

FIG. 2. Numerical solutions of KdV-equation, scheme (2.4) with $\eta = 0$, $\rho = 1.0$, $\varepsilon = 0.0005$, $N = 150$, $h = 0.04$, and $\tau = 0.001$. Initial condition: (2.6) with $H = 1.0$, $d_0 = 1.5$, $d_1 = 2.5$, and $b = 6.0$.

should increase linearly with H, and for small values of H the solution of the nonlinear equation should behave almost linearly. It is interesting that the amplitude of the wavepacket reaches a maximum value, with respect to H, and then decreases again.

Although the height H of the initial pulse has a marked effect on the amplitude of the wavepacket, further numerical experiments indicated that the width $d_1 - d_0$ of the initial pulse has no effect on this amplitude. In fact it seems that it is the presence of a discontinuity in the initial data which causes the wavepacket to appear and not the rectangular pulse as such. In an experiment where a discontinuous piecewise linear initial function was used instead of a piecewise constant one, the emergence of the same type of wavepacket was observed. In an experiment where the initial pulse was allowed to have steep-sloped sides, instead of being exactly rectangular, the amplitude of the emerging wavepacket was much smaller.

The amount of dispersion present in the numerical scheme also seems to be important. This can be controlled by varying ε, and it was found that for any value of h there is a certain ε-interval within which the wavepacket phenomenon is obtained. For values of ε which are too small, the wavepacket almost vanishes, and for values of ε which are too large, the wavepacket degenerates into a modulated wavetrain as in the linear case. For larger values of h this ε-interval shifts towards larger values of ε as well.

The specific type of nonlinearity in (2.1) also seems to be important. In addition to (2.1) we also considered the modified Korteweg–de Vries (MKdV) equation

$$u_t + \eta u_x + \rho u^2 u_x + \varepsilon u_{xxx} = 0 \tag{2.25}$$

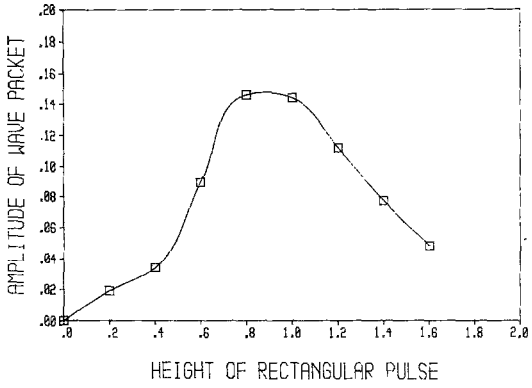

FIG. 3. The amplitude of the emerging saw-toothed wavepacket is shown against the height, H, of the rectangular pulse initial condition, for the KdV-equation, scheme (2.4). The following parameters were used: $\eta = 0$, $\rho = 1.0$, $\varepsilon = 0.0005$, $N = 150$, $h = 0.04$, and $\tau = 0.001$.

which we solved by the numerical scheme

$$\delta_n U_j^n + (\eta\tau/h)\,\delta_j U_j^n + (\rho\tau/3h)\,U_j^n(\mu_j U_j^n)(\delta_j U_j^n) + (\varepsilon\tau/h^3)\,\delta_j \Delta_j \nabla_j U_j^n = 0. \tag{2.26}$$

In this case, however, we were unable to observe a single wavepacket emerging from a rectangular pulse initial condition, no matter what values of ε and h we used. In all cases a modulate saw-toothed wavetrain, very similar to that observed in the linear case, preceded the solitons.

We cannot yet give a satisfactory explanation for this type of nonlinear modulation, but in the next section we shall point out some properties of this type of wavepacket, which we hope may be a beginning towards a more thorough analysis.

TABLE I

H	Amplitude of wavepacket
0.2	0.019
0.4	0.034
0.6	0.089
0.8	0.146
1.0	0.144
1.2	0.112
1.4	0.077
1.6	0.048

3. The Propagation of the Envelope of a Saw-toothed Wave Packet

Due to the nonlinear term in the KdV-equation, a Fourier analysis can no longer be applied to explain the appearance and propagation of saw-toothed solutions of the nonlinear numerical scheme. In the previous section it was shown by means of numerical experiments that such saw-toothed waves do exist in the nonlinear case and that they differ from their counterparts in the linear case, in the respect that they can emerge from discontinuous data as single wavepackets.

A different approach towards analyzing them is possible if we only concentrate on parasitic waves of wavelength $2h$ and consider the propagation of the *envelope* of such waves.

Our numerical experiments showed that the maximum amplitudes of the saw-toothed wave packets emerging from rectangular pulse initial data are relatively small. FromTable I and Fig. 3 it is seen that it is, for the parameters chosen, never larger than about 18% of the height of the initial pulse. In the next section we will report an experiment in which we used a saw-toothed wavepacket with a smooth envelope as an initial condition. Such a wavepacket became unstable when its amplitude was chosen to be too large, and it would propagate without too much distortion when it had a relatively small amplitude (not more than about 0.3 for the parameters used). We shall show below that our nonlinear analysis also breaks down when considering *large* amplitude wavepackets as solutions of (2.4).

In order to investigate the envelope of a modulated parasitic wave of wavelength $2h$, we consider a wave of the form

$$U_j^n = (-1)^j V_j^n, \tag{3.1}$$

where for each value of n, V_j^n is zero for all but a certain finite range of adjacent values of j. When we substitute (3.1) into the scheme (2.4), we find that V_j^n is a solution of

$$\delta_n V_j^n + (\tau/h)(4\varepsilon/h^2 - \eta)\,\delta_j V_j^n + (-1)^j \left(\frac{\rho\tau}{3h}\right)(\mu_j - 2)\, V_j^n \delta_j V_j^n + (\varepsilon\tau/h^3)\,\delta_j \Delta_j \nabla_j V_j^n = 0. \tag{3.2}$$

Note that (3.2) is a *nonlinear* difference equation which describes the propagation of the envelope of a saw-toothed wave of wavelength $2h$. This equation is clearly not a discrete analog of any partial differential equation, because of the presence of the factor $(-1)^j$ in the coefficient of the nonlinear term. For V_j^n sufficiently small, however, the nonlinear term may be neglected and V_j^n considered to be an approximate solution of the difference equation

$$\delta_n V_j^n + \{\tau(4\varepsilon - h^2\eta/h^3\}\,\delta_j V_j^n + (\varepsilon\tau/h^3)\,\delta_j \Delta_j \nabla_j V_j^n = 0. \tag{3.3}$$

We are, therefore, again considering the linear case of Section 2.1, but from a different viewpoint.

Assuming the existence of a smooth interpolate $v(x, t)$ of the discrete function V_j^n, such that $v(jh, n\tau) = V_j^n$, and performing a Taylor expansion about $(x, t) = (jh, n\tau)$, we find that $v(x, t)$ is a solution of the partial differential equation

$$v_t + \hat{\eta} v_x + \hat{\varepsilon} v_{xxx} = O(h^2) + O(\tau^2), \tag{3.4}$$

where

$$\begin{aligned} \hat{\eta} &= 4\varepsilon/h^2 - \eta \\ \hat{\varepsilon} &= 5\varepsilon/3 - \eta h^2/6. \end{aligned} \tag{3.5}$$

Thus (3.3) is seen to be consistent with the equation

$$v_t + \hat{\eta} v_x + \hat{\varepsilon} v_{xxx} = 0, \tag{3.6}$$

with a truncation error of the same order as that of scheme (2.4). Note also that, in the small amplitude limit we are now considering, the modulated saw-toothed wave (3.1) is an approximate solution of the linearized KdV-equation

$$u_t + \eta u_x + \varepsilon u_{xxx} = 0, \tag{3.7}$$

whereas its envelope is described by $v(x, t)$ which approximately satisfies *another* linearized KdV-equation, namely (3.6). This was not clear from the Fourier analysis in Section 2.1.

For small h, $\hat{\eta}$ is large ($\hat{\eta} = O(h^{-2})$) with respect to $\hat{\varepsilon}$, and the dispersion term $\hat{\varepsilon} v_{xxx}$ will be dominated by the convection term $\hat{\eta} v_x$ in (3.6). In the experiments reported in Section 2, ε (and consequently also $\hat{\varepsilon}$) was usually taken to be very small ($\varepsilon = O(h^2)$), and thus Eq. (3.4) effectively becomes

$$v_t + \hat{\eta} v_x = O(h^2) + O(\tau^2) \tag{3.8}$$

with

$$\hat{\eta} = O(1).$$

Equation (3.8) represents a wavepacket with an envelope being propagated at the speed $\hat{\eta}$, which is, according to (3.5) and (2.24b), equal to the linear group velocity of a saw-toothed wave solution of the numerical scheme. This is well in agreement with the observed behavior of the saw-toothed wave packets emerging from rectangular pulse initial conditions.

The fact that a smooth interpolate of V_j^n, approximately satisfying some partial differential equation, cannot be found when the nonlinear term is retained in (3.2), together with our numerical experiments indicating the instability of large amplitude saw-toothed wave packets, lead us to suspect that all such wavepackets occurring in the solution of (2.4) must be of small amplitude and, therefore, essentially linear in character.

It will be recalled that it was the presence of the factor $(-1)^j$ in (3.2) which made it impossible to obtain a continuized version of this discrete equation if the nonlinear term was retained. This factor appears because the nonlinearity is *quadratic*. If the nonlinearity were cubic, as in the case of the MKdV-equation (1.2), a similar analysis would yield a difference equation which can be continuized. Thus with a cubic nonlinearity this type of analysis could be carried much further and could be applied to wave packets with much larger amplitudes.

In Section 4 we will report numerical experiments in which we used single saw-toothed wave packets as initial conditions with the scheme (2.26) for the MKdV-equation. We did in fact find that, unlike the case of the KdV, the amplitudes of such wave packets could be made relatively large.

To apply the analysis of this section to the scheme (2.26) for the MKdV-equation, we substitute (3.1) into (2.26) to obtain

$$\delta_n V_j^n + (\tau/h)(4\varepsilon/h^2 - \eta)\,\delta_j V_j^n + (\rho\tau/3h)\,V_j^n(\mu_j - 2)\,V_j^n\,\delta_j V_j^n + (\varepsilon\tau/h^3)\,\delta_j \Delta_j \nabla_j V_j^n = 0. \tag{3.9}$$

Assuming the existence of an interpolate $v(x, t)$ such that $v(jh, n\tau) = V_j^n$ and performing a Taylor analysis about $(x, t) = (jh, n\tau)$ we find that $v(x, t)$ is a solution of

$$v_t + \hat{\eta} v_x + \hat{\rho} v^2 v_x + \hat{\varepsilon} v_{xxx} = O(h^2) + O(\tau^2), \tag{3.10}$$

where

$$\begin{aligned} \hat{\eta} &= 4\varepsilon/h^2 - \eta \\ \hat{\rho} &= \rho/3 \\ \hat{\varepsilon} &= 5\varepsilon/3 - \eta h^2/6. \end{aligned} \tag{3.11}$$

In this case (3.1) is an approximate saw-toothed wave solution of the MKdV-equation

$$u_t + \eta u_x + \rho u^2 u_x + \varepsilon u_{xxx} = 0 \tag{3.12}$$

while its envelope is described by a function $v(x, t)$ which approximately satisfies another MKdV-equation, namely (3.10). Thus a saw-toothed wavepacket having an envelope with properties approaching that of a MKdV-soliton, is therefore a distinct possibility. The single soliton solution of the MKdV-equation (3.10) is of the form

$$v(x, t) = (6\hat{\varepsilon}/\rho)^{1/2}\,\beta[\operatorname{sech} \beta(x - \hat{\eta}t - \hat{\varepsilon}\beta^2 t - x_0)], \tag{3.13}$$

where β is a real parameter [13].

Thus if we put

$$V_j^0 = (6\hat{\varepsilon}/\hat{\rho})^{1/2}\beta \operatorname{sech}[\beta(hj - x_0)]$$

in (3.1), we would expect to observe a wavepacket which does not change its shape appreciably, and maintain a velocity of $\hat{\eta} + \hat{\varepsilon}\beta^2$. If we choose V_j^0 consistent with an N-soliton solution of the MKdV-equation (3.10), it should be possible to observe interactions of wavepacket "solitons." The results of such numerical experiments are reported in the next section.

A question which also arises is: What will happen when a true soliton of the MKdV-equation and a wave packet "soliton" of the same equation interacts? The same might be asked with respect to a true soliton of the KdV-equation and a KdV wave packet (which is quite different from a soliton). In the next section we shall report some numerical experiments which shows markedly different results for these two cases.

4. Numerical Experiments

It was shown in the previous section that a saw-toothed wavepacket soliton solution is not possible for the KdV-equation, but that such wave packets travel with velocity very nearly equal to $4\varepsilon/h^2 - \eta$ and show some dispersion. When h is small, however (with $\eta = 0$), the velocity is large in comparison with the rate at which dispersion is introduced and the wavepacket is propagated initially with little change in the shape of the envelope.

Figure 4 shows the solution of the Zabusky–Kruskal scheme, (2.4), with

$$\eta = 0 \qquad \rho = 1 \qquad \varepsilon = 0.0005$$
$$N = 150 \qquad h = 0.04 \qquad \tau = 0.002 \qquad b = 6.$$

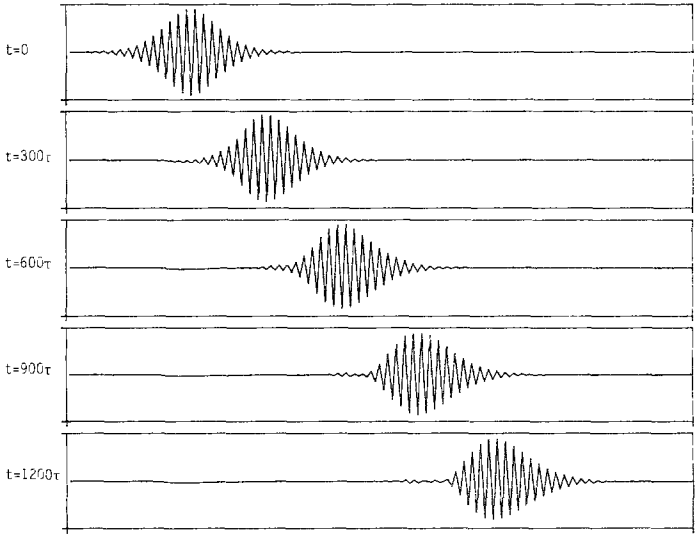

FIG. 4. Numerical solution of KdV-equation, scheme (2.4) with $\eta = 0$, $\rho = 1.0$, $\varepsilon = 0.0005$, $N = 150$, $h = 0.04$, and $\tau = 0.002$. Initial condition: (4.1) with $\hat{\rho} = 0.33333333$, $\hat{\varepsilon} = 0.0008333333$, $\beta = 3.0$, and $x_0 = 1.2$.

A graph of the solution was drawn every 300 time steps from the 0th to the 1200th time step. Each graph is shown for the intervals $x \in [0.0, 6.0]$ and $U \in [-0.3, 0.3]$. The initial condition used was

$$U_j^0 = (-1)^j \frac{12\hat{\varepsilon}\beta^2}{\hat{\rho}} \operatorname{sech}^2(\beta(hj - x_0)) \qquad \text{for} \quad j \in \mathbb{N} \cap [1, 150] \tag{4.1}$$

with

$$\hat{\rho} = \frac{\rho}{3} = \frac{1}{3}$$

$$\hat{\varepsilon} = \frac{5\varepsilon}{3} - \frac{\eta h^2}{6} = \frac{1}{1200}$$

$$\beta = 3.0, \qquad x_0 = 1.2$$

According to (3.11) the group velocity of such a wavepacket is

$$\hat{\eta} = \frac{4\varepsilon}{h^2} - \eta = 1.25.$$

The center of the wavepacket initially was at 1.2 and, after a time of 2.4 units, it was approximately at 4.18, thus giving an experimental velocity of 1.24.

It was also shown in the previous section that a wavepacket soliton solution is

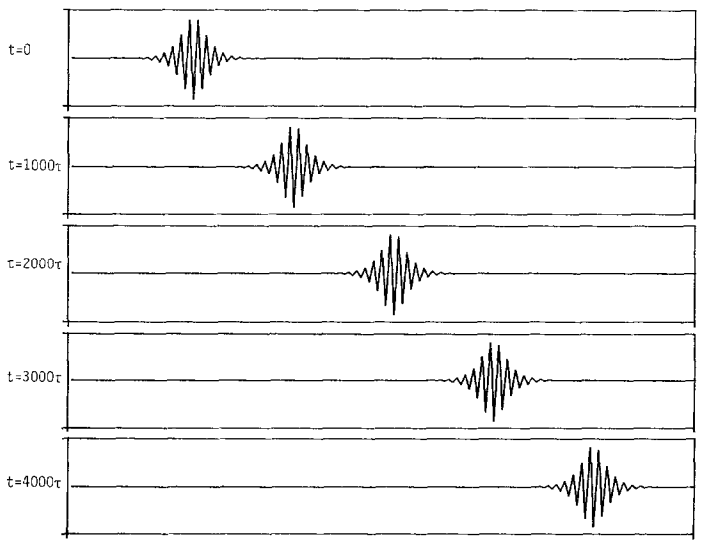

FIG. 5. Numerical solution of MKdV-equation, scheme (2.26) with $\eta = 12.5$, $\rho = 1.0$, $\varepsilon = 0.005$, $N = 150$, $h = 0.04$, and $\tau = 0.002$. Initial condition: (4.2) with $\hat{\rho} = 0.33333333$, $\hat{\varepsilon} = 0.005$, $\beta = 10.0$, and $x_0 = 1.2$.

possible for the MKdV-equation. Figure 5 shows the solution of the scheme (2.26), with

$$\eta = 12.5 \qquad \rho = 1 \qquad \varepsilon = 000.5$$
$$N = 150 \qquad h = 0.04 \qquad \tau = 0.002 \qquad b = 6.$$

A graph of the solution was drawn every 1000 time steps, from the 0th to the 4000th time step. Each graph is shown for the intervals $x \in [0.0, 6.0]$ and $U \in [-3.5, 3.5]$. The initial condition used was

$$U_j^0 = (-1)^j \sqrt{6\hat{\varepsilon}/\hat{\rho}}\, \beta \operatorname{sech}(\beta(hj - x_0)) \qquad \text{for} \quad j \in \mathbb{N} \cap [1, 150] \tag{4.2}$$

with

$$\hat{\rho} = \frac{\rho}{3} = \frac{1}{3}$$
$$\hat{\varepsilon} = \frac{5\varepsilon}{3} - \frac{\eta h^2}{6} = 0.005$$
$$\beta = 10, \qquad x_0 = 1.2;$$

η was chosen such that $\hat{\eta} = 0$, thus the velocity of the wavepacket soliton is solely due to its solitonic nature with no translational velocity added.

The results of the experiment show that the wavepacket soliton travelled very stably with constant velocity and with no appreciable change of shape for 4000 time steps. This confirms the validity of the envelope approach of Section 3, for the MKdV-equation.

According to (3.14) the velocity of the wavepacket soliton, should be

$$\hat{\eta} + \hat{\varepsilon}\beta^2 = 0.5.$$

In this experiment the center of the wavepacket soliton has moved from 1.2 to approximately 5.04 in 8 time units, giving an experimental velocity of 0.48.

It was also found that the solution of the scheme (2.26) with true soliton initial conditions often became unstable and decayed into a highly oscillatory solution leading to a nonlinear blowup shortly afterwards. This occurred more frequently when the β-parameter was large. The wavepacket soliton seemed to be a much more stable solution of (2.26), than true solitons.

Figure 6 shows the results of an experiment where a KdV-wavepacket and a KdV-soliton were allowed to collide. The scheme (2.4) was solved with

$$\eta = 0.0 \qquad \rho = 1.0 \qquad \varepsilon = 0.0005$$
$$N = 150 \qquad h = 0.04 \qquad \tau = 0.002 \qquad b = 6.0.$$

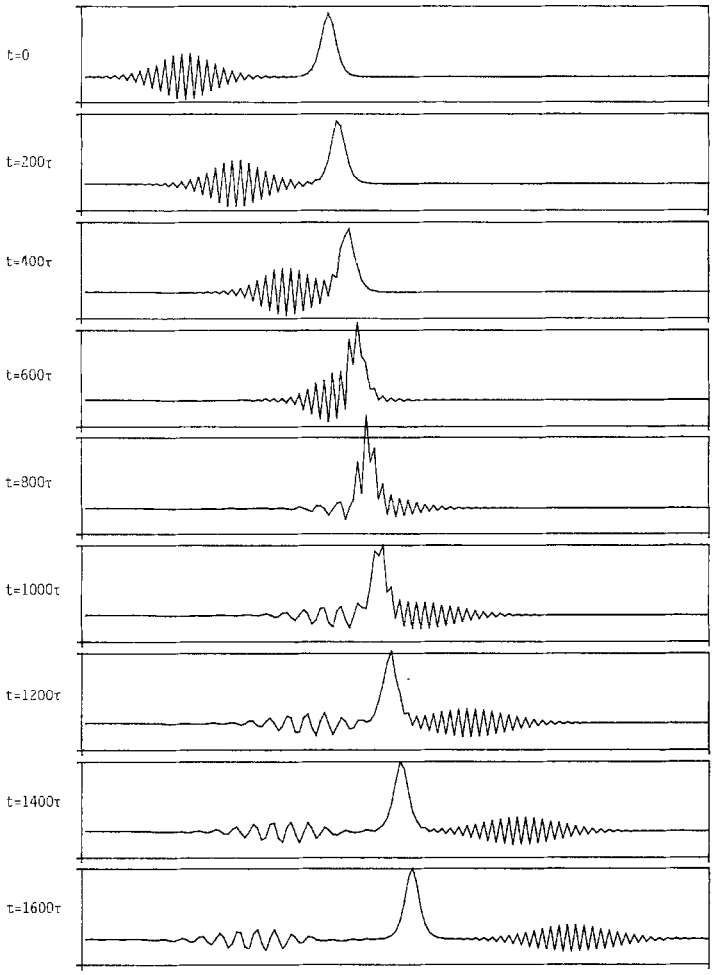

FIG. 6. Numerical solution of KdV-equation, scheme (2.4) with $\eta = 0.0$, $\rho = 1.0$, $\varepsilon = 0.0005$, $N = 150$, $h = 0.04$, and $\tau = 0.002$. Initial condition: (4.3) with $\hat{\rho} = 0.33333333$, $\hat{\varepsilon} = 0.000833333$, $\beta_0 = 3.0$, $x_0 = 1.00$, $\beta_1 = 11.0$, and $x_1 = 2.36$.

A graph of the solution was drawn every 200 time steps from the 0th to the 1600th time step. Each graph is shown for the intervals $x \in [0.0, 6.0]$ and $U \in [-0.3, 0.8]$. The initial condition used was simply a linear superposition of the wavepacket and the soliton placed far enough apart,

$$U_j^0 = (-1)^j \frac{12\varepsilon\beta_0^2}{\hat{\rho}} \operatorname{sech}^2(\beta_0(hj - x_0)) + \frac{12\varepsilon\beta_1}{\rho} \operatorname{sech}^2(\beta_1(hj - x_1)) \quad \text{for } j \in \mathbb{N} \cap [1, 150] \tag{4.3}$$

with ρ and ε as given above, and

$$\hat{\rho} = \frac{\rho}{3} = \frac{1}{3}$$

$$\hat{\varepsilon} = \frac{5\varepsilon}{3} - \frac{\eta h^2}{6} = \frac{1}{1200}$$

$$\beta_0 = 3.0, \qquad x_0 = 1.0$$

$$\beta_1 = 11.0, \qquad x_1 = 2.36.$$

The results are interesting and surprising, but still lack an explanation. After the collision the soliton emerged with larger amplitude, and the wavepacket emerged with smaller amplitude, still travelling to the right at approximately the predicted velocity of 1.25. In addition, a third localized solution appeared: a wavepacket with smaller wave number than the incident saw-toothed wavepacket, and travelling to the left with constant velocity.

A number of such collision experiments were done. In general, it was found that the soliton always emerged with an increased amplitude (in the order of 10%). It also appeared that solitons with large amplitude, with respect to the amplitude of the incident wavepacket, had a more destructive effect on the wavepacket: The larger the amplitude of the soliton, the smaller the amplitude of the transmitted wavepacket and the larger the amplitude of the reflected wavepacket.

Similar collision experiments were done for the MKdV-scheme (2.26). Figure 7 shows the solution of (2.26) with

$$\eta = 0.0 \qquad \rho = 1.0 \qquad \varepsilon = 0.002$$

$$N = 150 \qquad h = 0.04 \qquad \tau = 0.002 \qquad b = 6.0.$$

A graph of the solution was drawn every 50 time steps from the 0th to the 400th time step. Each graph is shown for the intervals $x \in [0.0, 6.0]$ and $U \in [-1.2, 1.2]$. The initial condition used was

$$U_j^0 = (-1)^j \sqrt{6\hat{\varepsilon}/\hat{\rho}}\, \beta_0 \operatorname{sech}(\beta_0(hj - x_0)) + \sqrt{6\varepsilon/\rho}\, \beta_1 \operatorname{sech}(\beta_1(hj - x_1)) \quad \text{for} \quad j \in \mathbb{N} \cap [1, 150] \tag{4.4}$$

with ρ and ε as given above and

$$\hat{\rho} = \frac{\rho}{3} = \frac{1}{3}$$

$$\hat{\varepsilon} = \frac{5\varepsilon}{3} - \frac{\eta h^2}{6} = \frac{1}{300}$$

$$\beta_0 = 4.0 \qquad x_0 = 1.0$$

$$\beta_1 = 9.0 \qquad x_1 = 2.68.$$

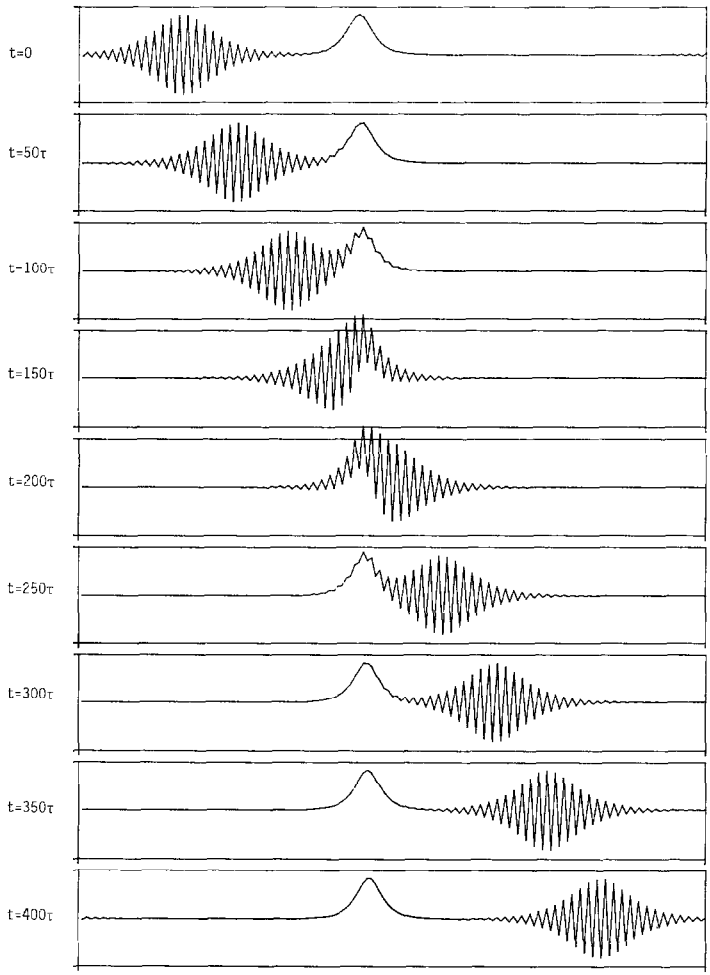

FIG. 7. Numerical solution of MKdV-equation, scheme (2.26) with $\eta = 0.0$, $\rho = 1.0$, $\varepsilon = 0.002$, $N = 150$, $h = 0.04$, and $\tau = 0.002$. Initial condition: (4.4) with $\hat{\rho} = 0.33333333$, $\hat{\varepsilon} = 0.003333333$, $\beta_0 = 4.0$, $x_0 = 1.00$, $\beta_1 = 9.0$, and $x_1 = 2.68$.

The results show that in the case of the scheme(2.26) for the MKdV-equation, a collision between the wavepacket soliton and the true soliton produced no side effects: The two types of solitons passed through each other as in the case of a linear equation. Even the usual phase shift resulting from an interaction between two true solitons of the MKdV-equation is unobservable in this case.

In the following two expriments two saw-toothed wavepacket solitons of the MKdV-equation were allowed to collide. Figure 8 shows the solution of the scheme (2.26), where both the saw-toothed solitons has the upper parts of their envelopes supported by the even nodes and the lower parts by the odd nodes. Figure 9 shows

the results of a similar experiment, where the first saw-toothed soliton has its upper envelope supported by the even nodes and the second has its upper envelope supported by the odd nodes. The following parameters were used:

$$\eta = 12.5 \qquad \rho = 1.0 \qquad \varepsilon = 0.005$$
$$N = 150 \qquad h = 0.04 \qquad \tau = 0.002 \qquad b = 6.0.$$

The initial condition used in these experiments was

$$U_j^0 = (-1)^j \sqrt{6\hat{\varepsilon}/\hat{\rho}}\,[\beta_0 \operatorname{sech}(\beta_0(hj - x_0)) \pm \beta_1 \operatorname{sech}(\beta_1(hj - x_1))] \quad \text{for } j \in \mathbb{N} \cap [1, 150] \tag{4.5}$$

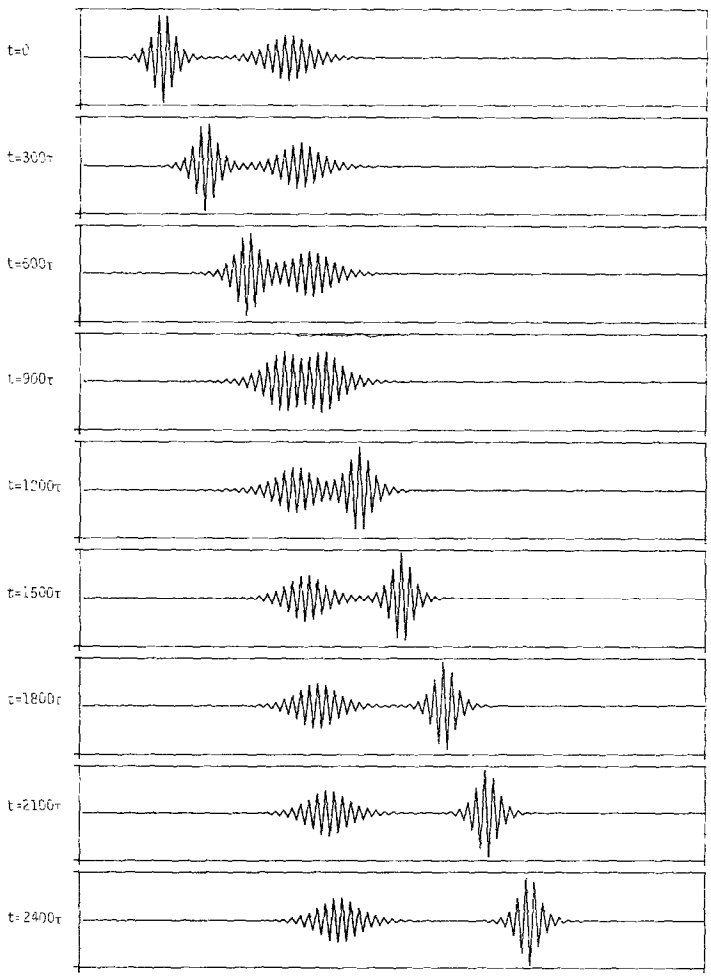

FIG. 8. Numerical solution of MKdV-equation, scheme (2.26) with $\eta = 12.5$, $\rho = 1.0$, $\varepsilon = 0.005$, $N = 150$, $h = 0.04$, and $\tau = 0.002$. Initial condition: (4.5) with + sign and with $\hat{\rho} = 0.33333333$, $\hat{\varepsilon} = 0.005$, $\beta_0 = 12.0$, $x_0 = 0.8$, $\beta_1 = 6.0$, and $x_1 = 2.0$.

with

$$\hat{\rho} = \frac{\rho}{3} = \frac{1}{3}$$

$$\hat{\varepsilon} = \frac{5\varepsilon}{3} - \frac{\eta h^2}{6} = 0.005$$

$$\beta_0 = 12.0 \qquad \beta_1 = 6.0.$$

In Fig. 8, x_0 and x_1 were chosen as

$$x_0 = 0.8 \qquad x_1 = 2.0$$

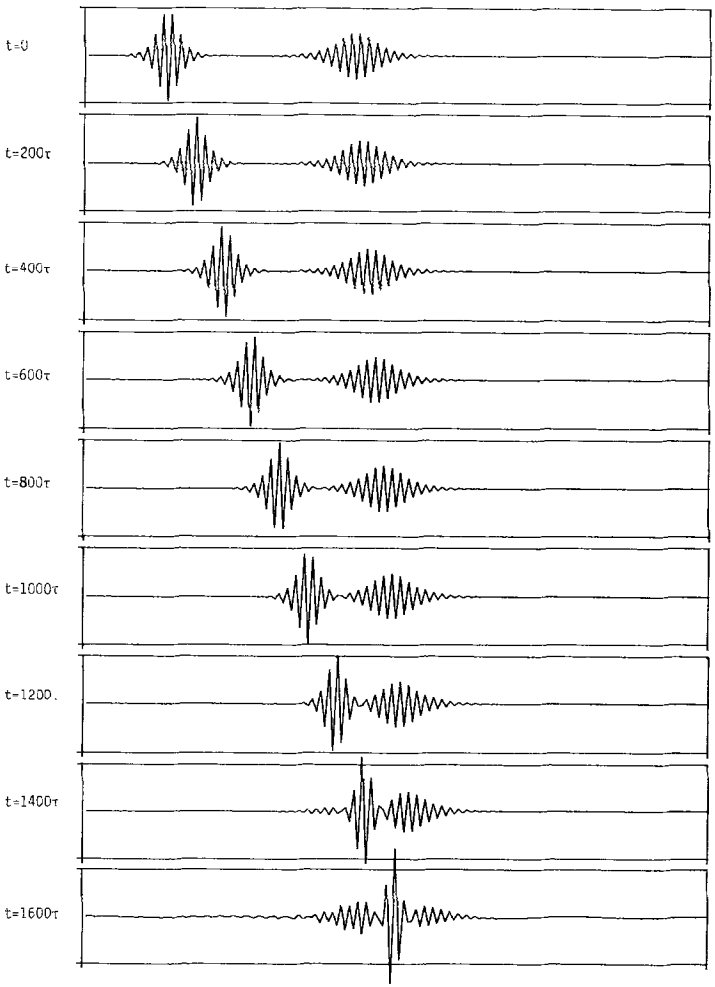

FIG. 9. Numerical solution of MKdV-equation, scheme (2.26) with $\eta = 12.5$, $\rho = 1.0$, $\varepsilon = 0.005$, $N = 150$, $h = 0.04$, and $\tau = 0.002$. Initial condition: (4.5) with $-$ sign and with $\hat{\rho} = 0.33333333$, $\hat{\varepsilon} = 0.005$, $\beta_0 = 12.0$, $x_0 = 0.8$, $\beta_1 = 6.0$, and $x_1 = 2.6$.

and the + sign was taken in (4.5). A graph of the solution was drawn every 300 time steps from the 0th to the 2400th time step. Each graph is shown for the intervals $x \in [0.0, 6.0]$ and $U \in [-3.8, 3.8]$.

In Fig. 9, x_0 and x_1 were chosen as

$$x_0 = 0.8 \qquad x_1 = 2.6$$

and the − sign was taken in (4.5). A graph of the solution was drawn every 200 time steps from the 0th to the 1600th time step. Each graph is shown for the intervals $x \in [0.0, 6.0]$ and $U \in [-3.8, 3.8]$.

Figure 8 shows a typical two-soliton interaction with the usual phase shift. In Fig. 9, the development of a nonlinear instability is witnessed. The solution blows up between the 1600th and 1800th time steps. Such a nonlinear instability is not totally unexpected, since energy is not conserved by the scheme (2.26).

It is evident, however, from there experiments that interacting saw-toothed solitons are possible for the discrete version of the MKdV, provided that the interacting solitons all have upper envelopes with support on either the even or the odd nodes. This means that the saw-toothed carrier waves of the two wavepacket solitons should have the same phase.

5. Conclusions

In the preceding sections we have shown that, with rectangular pulse initial data, discretized versions of both the KdV- and MKdV-equations have high wave number components in their solutions which are not present in the analytical solutions of these equations.

In the case of the KdV-equation, this can take the form of a small solitary saw-toothed wave packet, moving at a velocity very nearly equal to the linear group velocity, with little dispersion. Because of their relatively small amplitudes, the propagation of these wave packets is essentially governed by a linearized KdV-equation. Attempts to find stable wave packet solutions, with envelopes large enough for nonlinear effects to come into play, failed.

In the case of the MKdV-equation the parasitic high wave number components emerging from an initial rectangular pulse took the form of a modulated wave train, as in the case of a linearized KdV-equation. The numerical scheme for this equation, however, does admit saw-toothed wavepacket solutions, with no apparent restriction on its amplitude. The envelope of such a wavepacket approximately satisfies *another* MKdV-equation, and wavepackets behaving like solitons can be constructed.

It is remarkable that, in spite of the fact that saw-toothed MKdV-"solitons" are much more stable during interactions than the wavepackets of the KdV-equation, it is in the latter case that solitary wavepackets are seen to emerge from a rectangular

mechanism of nonlinear modulation, a further investigation is necessary.

It should also be interesting to investigate discrete versions of other dispersive nonlinear wave equations, in order to see whether similar phenomena can be observed in such cases.

REFERENCES

1. G. W. HEDSTROM, *SIAM J. Numer. Anal.* **16**, 385 (1979).
2. S. W. SCHOOMBIE, Report NA/43, Dept. of Mathematics, Univ. of Dundee, 1980 (unpublished).
3. L. N. TREFETHEN, *SIAM Rev.* **24**, 113 (1982).
4. L. N. TREFETHEN, *J. Comput. Phys.* **49**, 199 (1983).
5. L. N. TREFETHEN, *Commun. Pure Appl. Math.* **37**, 329 (1984).
6. M. B. GILES AND W. T. THOMPKINS, *J. Comput. Phys.* **58**, 349 (1985).
7. G. B. WHITHAM, *Linear and Nonlinear Waves* (Wiley, New York, 1974).
8. N. J. ZABUSKY AND M. D. KRUSKAL, *Phys. Rev. Lett.* **15**, 240 (1965).
9. P. L. BHATNAGAR, *Nonlinear Waves in One-Dimensional Dispersive Systems* (Oxford Univ. Press (Clarendon), Oxford, 1979).
10. J. M. SANZ-SERNA, *J. Comput. Phys.* **47**, 199 (1982).
11. A. C. NEWELL, *SIAM J. Appl. Math.* **33**, 133 (1977).
12. I. S. GREIG AND J. L. MORRIS, *J. Comput. Phys.* **20**, 64 (1976).
13. R. K. DODD, J. C. EILBECK, J. D. GIBBON, AND H. C. MORRIS, *Solitons and Nonlinear Wave Equations* (Academic Press, London, 1982).